

Synthesis of the [Ga]-MFI under Atmospheric Pressure

Jinu Park, Sang-Bum Kim, Jae-Mok Ha*, Myung-Soo Kim, Hong-Soo Park and Hyun-Sik Hahm†

Department of Chemical Engineering, Myongji University, Yongin 449-728, Korea

*Agency for Technology and Standards, Kwacheon 427-716, Korea

(Received 14 March 2001 • accepted 24 April 2001)

Abstract—The crystallization of the [Ga]-MFI was investigated as a function of synthesis time under atmospheric pressure. The molar composition of the reactants was $100\text{SiO}_2\text{-Ga}_2\text{O}_3\text{-}11\text{Na}_2\text{O-}1\text{TPABr-}3500\text{H}_2\text{O}$. The crystallinity of the [Ga]-MFI was examined by using several analytical instruments, such as XRD, XPS, XRF, FT-IR, solid-state *mas*-NMR, DTG/DTA, and SEM. The [Ga]-MFI was successfully synthesized under atmospheric pressure at 97°C in 72 h. It was found that the nucleation of the [Ga]-MFI took a quite long time, but the crystallization took place very fast. It is supposed that nucleation is the rate-controlling step in the [Ga]-MFI synthesis under atmospheric pressure. Consequently, if the induction period of the nucleation can be shortened, it would be possible to synthesize the [Ga]-MFI commercially under atmospheric pressure.

Key words: Zeolite, [Ga]-MFI, Gallosilicate, Atmospheric Pressure Synthesis, ^{71}Ga -*mas*-NMR

INTRODUCTION

The [Ga]-MFI is a zeolite that is prepared by the substitution of Ga for Al in the framework of ZSM-5. The [Ga]-MFI shows high activity and selectivity in the aromatization of lower alkanes, which is a process of great commercial importance [Lee et al., 1986; Guisnet et al., 1992; Giannetto et al., 1993; Choudhary et al., 1996; Lee et al., 1998; Kim et al., 2001]. There are several reported methods to incorporate Ga into the MFI zeolite: ion exchange [Gnep et al., 1989; Khodakov et al., 1990], impregnation [Bayense et al., 1991; Meriaudeau and Naccache, 1990], physical mixing of Ga_2O_3 with MFI zeolite [Gnep, 1998; Yakerson et al., 1989], and partial or full substitution of Ga for Al of the MFI zeolite [Thomas and Liu, 1986; Choudhary et al., 1996; Simmons et al., 1987; Inui et al., 1987; Kanai and Kawata, 1989; Mobil Oil Co., 1986, 1989; Mitsubishi Chem. Co., 1997; Chiyoda Co., 1993; Vaw ver Aluminium Werke Ag., 1992]. Recently, the last method has drawn interest because of the even distribution of gallium, which exhibits higher dehydrogenation activity. Until now, the [Ga]-MFIs have been synthesized by using autoclaves under an autogenous pressure above 150°C [Giannetto et al., 1993; Choudhary and Kinage, 1997].

In this study, the synthesis of the [Ga]-MFI type zeolite was conducted using a Teflon reactor under atmospheric pressure, and the crystallization of the [Ga]-MFI was also investigated.

EXPERIMENTAL

1. Synthesis of the [Ga]-MFI

The materials for the [Ga]-MFI synthesis were Ludox-AS40 as a silica source (Du Pont Chem. Co.), $\text{Ga}(\text{NO}_3)_3$ as a Ga source (Aldrich Chem. Co.; 99.9%), NaOH as an alkali source (Junsei Chem. Co.), and *tetra*-propyl ammonium bromide (TPABr) as an organic template (Dongkyung Hwasung Co.).

The [Ga]-MFI was synthesized under atmospheric pressure in a 1.5 L Teflon reactor equipped with a condenser and stirrer, and the reactor was heated with an oil bath. The molar composition of the reactants was $100\text{SiO}_2\text{-Ga}_2\text{O}_3\text{-}11\text{Na}_2\text{O-}1\text{TPABr-}3500\text{H}_2\text{O}$. The synthesis procedures are as follows. First, 640 g of Ludox-AS40, 50.48 g

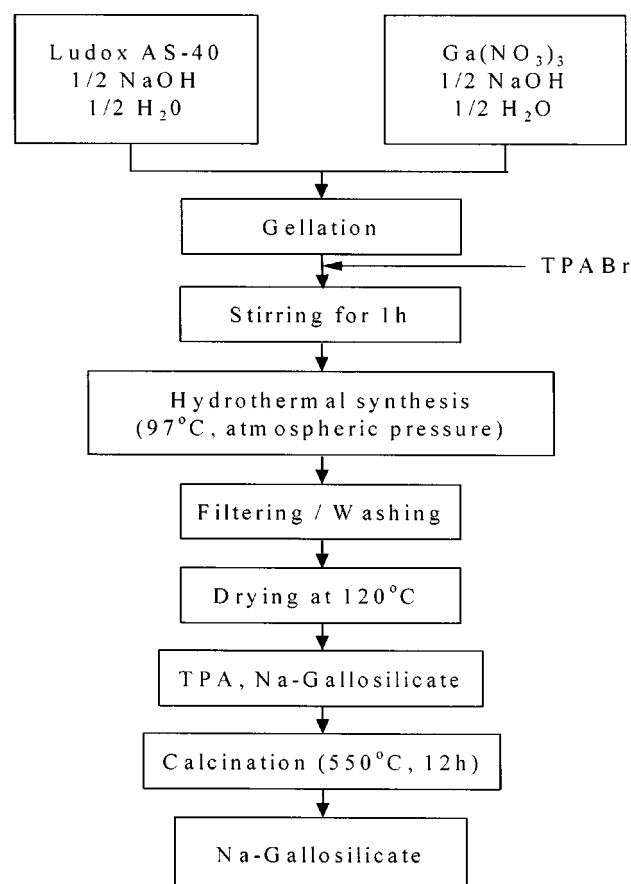


Fig. 1. Flowsheet for the synthesis of the [Ga]-MFI.

†To whom correspondence should be addressed.

E-mail: hahm@mju.ac.kr

of 50 wt%-NaOH solution, and 1,116 g of distilled water were mixed in a propylene beaker (I). Then, 1,116 g of distilled water, 50.48 g of 50 wt%-NaOH solution, and 21.84 g of gallium (III) nitrate hydrate were poured in another propylene beaker (II) and mixed well. Next, the solution of the beaker (II) was slowly poured into the beaker (I) with a vigorous stirring. Finally, 124.8 g of *tetra*-propylene ammonium bromide (TPABr) was added to the mixture. The obtained mixture was then poured into the reactor mentioned above, and the reaction was carried out at 97 °C and under atmospheric pressure with stirring (300 rpm). The flowsheet for the synthesis of the [Ga]-MFI is shown in Fig. 1. ZSM-5 was also synthesized by the same procedure mentioned above to compare with the [Ga]-MFI produced.

2. Characterizations

In order to investigate the crystallization of the [Ga]-MFI, the reaction was stopped after a predetermined reaction time, and the reactor was quenched. Then, the content of the reactor was filtered with a membrane filter of 0.1 µm, and washed with distilled water until the filtrate became neutral. The obtained solids were dried at 100 °C overnight and reserved in a desiccator. The obtained solids were calcined raising temperature at a rate of 5 °C/min to 550 °C with a flow of 50 ml air/min.

The solids were then characterized by XRD (Siemens, D5005), FT-IR (Nicolet, Impact 400), solid state *mas*-NMR (Varian, Plus300), XPS (ESCALAB, 220i), SEM (Shimatsu, Alpha 25a), XRF (Rigaku, 3270), and DTG/DTA (SETARAM92-16.18).

RESULTS AND DISCUSSION

1. Composition Change

The composition and physico-chemical properties of the [Ga]-MFI zeolites prepared were characterized by using XRF and XPS, and the results are summarized in Table 1. Except for the initial gel formation state, the molar ratios of Si to Ga₂ between the surface and the bulk were almost the same. This result reveals that the crystallization of the [Ga]-MFI takes place homogeneously, indicating the uniform distribution of Ga throughout the zeolite framework.

In Table 1, three XPS peaks of Ga (2p) are observed at 1119.7,

1118.9, and 1117.8 eV at the initial state, while only one peak is observed at 1119.2 eV after 72 h of reaction. This result suggests that the Ga species were three kinds in the initial state, but it became one kind after 72 h of reaction. The binding energy of 1119.2 eV of Ga (2p) of the final product is higher than those of Ga (1117 eV) and Ga₂O₃ (1117.7 eV). This reveals that the gallium existing in the lattice of the [Ga]-MFI is GaO₄⁻ tetrahedral form, so the gallium can have a higher oxidation number [Shpiro et al., 1994].

2. Structure Change during the Crystallization

The structure changes of the products with synthesis time were investigated by using several analytical instruments. The formation of the unit cell structure of the [Ga]-MFI was identified by FT-IR; the crystallinity and phase changes with synthesis time were by XRD; the gallium and silicon species existing in the [Ga]-MFI framework were by ⁷¹Ga- and ²⁹Si-*mas*-NMR; and the straight- and sinusoidal-type channels that are a unique structure of MFI-type zeolite were by ¹³C-*cpmas*-NMR.

2-1. FT-IR

Using FT-IR, one can easily identify the five-member ring and double five-member ring of the MFI-type zeolite as well as its unit cell structure. The MFI-type zeolites exhibit their unique IR peaks in the regions of 1,220 and 550 cm⁻¹ [Szostak, 1988; Cambor, 1992]. The IR spectra of the products with synthesis time are presented in Fig. 2. Peaks in the regions of 1,220 and 550 cm⁻¹, corresponding to the five-member ring and double five-member ring (D5R), were observed after 32 h of reaction, and a new peak around 970 cm⁻¹, which is not observed in ZSM-5 and silicalite, was observed. On and after 63 h of reaction, the peak for a T-O bonding (attributed by the internal vibration of tetrahedral TO₄) shifted from 475 cm⁻¹ to 450 cm⁻¹. A similar phenomenon was also observed in the XPS result listed in Table 1, in which the binding energy of O(1s) shifted from 531.9 (initial) to 532.7 eV (after 63 h). As can be seen in Fig. 2, the peaks for the external linkage vibration of five-member ring and D5R were observed at 1220 and 550 cm⁻¹, respectively, beyond 63 h of reaction. Consequently, it would appear that the shift of the T-O wave number and the change of the binding energy of O(1s) stemmed from a change in the environment of the TO₄, which was caused by the formation of the crystalline structure due to the con-

Table 1. Physico-chemical properties of the synthesized [Ga]-MFI as a function of synthesis time

Synthesis time (h)	Analysis by XRF (wt%)					Analysis by XPS			
	SiO ₂	Ga ₂ O ₃	Na ₂ O	Mole ratio		Mole ratio of SiO ₂ /Ga ₂ O ₃	Binding energy (eV)*		
				SiO ₂ /Ga ₂ O ₃	Na ₂ O/Ga ₂ O ₃		Ga2p ₃	O1s	Si2p
Initial	93.4	2.78	3.58	105.2	3.9	165.4	1119.7 1118.9 1117.8	531.9	103.8
32	94.8	2.86	2.08	103.3	2.2	-	-	-	-
60	94.7	2.95	2.12	100.5	2.2	-	-	-	-
63	94.8	2.88	2.01	102.6	2.1	104.2	1120.4 1119.1	532.7	104
66	94.9	2.91	1.97	102.1	2.0	103.1	1119.2	532.7	104
69	95.4	2.83	1.56	105.3	1.7	-	-	-	-
72	95.3	2.91	1.54	102.5	1.6	102.4	1119.2	532.7	104

Initial mole ratios of the reactants : SiO₂/Ga₂O₃=100; SiO₂/Na₂O=9; SiO₂/TPA₂O=9; and H₂O/SiO₂=35.

*: Referenced to the C(1s) of 285±0.2 eV.

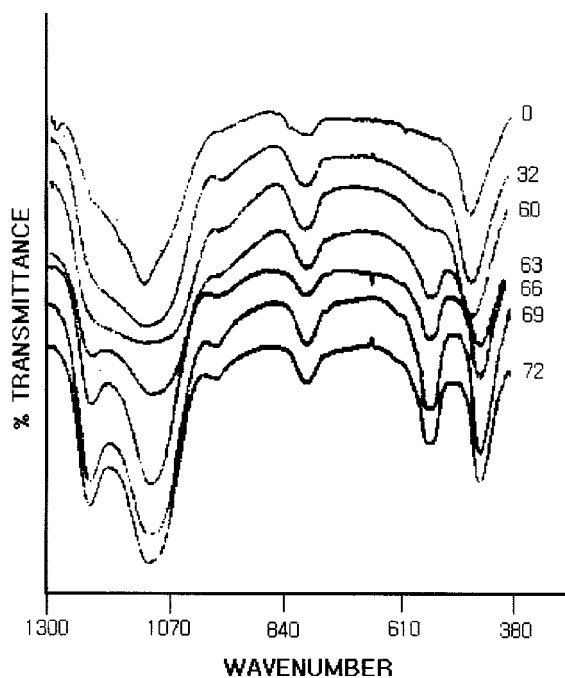


Fig. 2. FT-IR spectra for products as a function of synthesis time.

densation of SBU (secondary building unit) and chains formed from PBU (primary building unit). It is concluded that the final products are the MFI structure by the unique peaks observed at 454, 547, 794, 1,110, and 1,220 cm^{-1} .

2-2. X-ray Diffraction

The phases of the products ([Ga]-MFI) were identified by using XRD as a function of the synthesis time. In order to compare the structures of the products with ZSM-5, which has the same structure with [Ga]-MFI, ZSM-5 was also synthesized under the same synthesis condition. The XRD patterns for [Ga]-MFI and ZSM-5

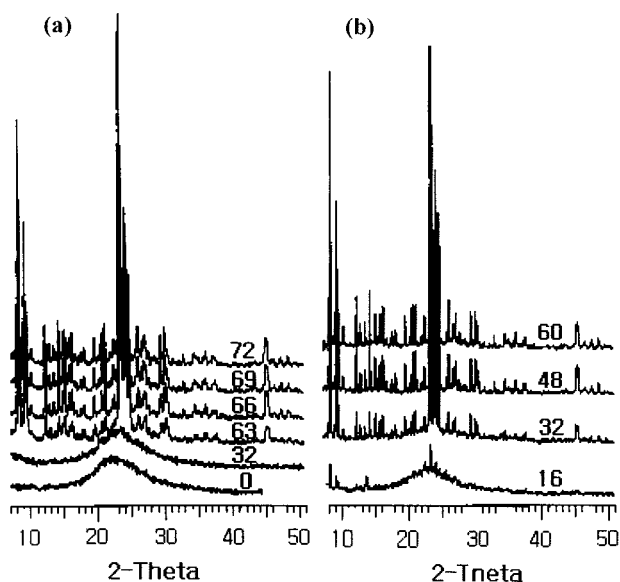


Fig. 3. X-ray diffraction patterns for products as a function of synthesis time.

(a) [Ga]-MFI, (b) ZSM-5

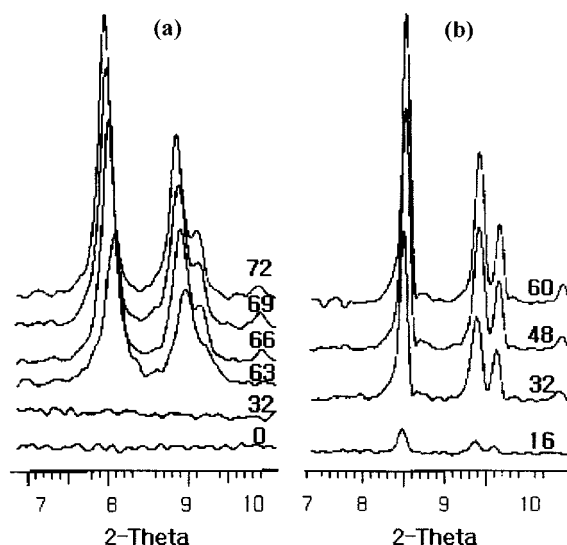


Fig. 4. X-ray diffraction patterns for products as a function of synthesis time.

(a) [Ga]-MFI, (b) ZSM-5

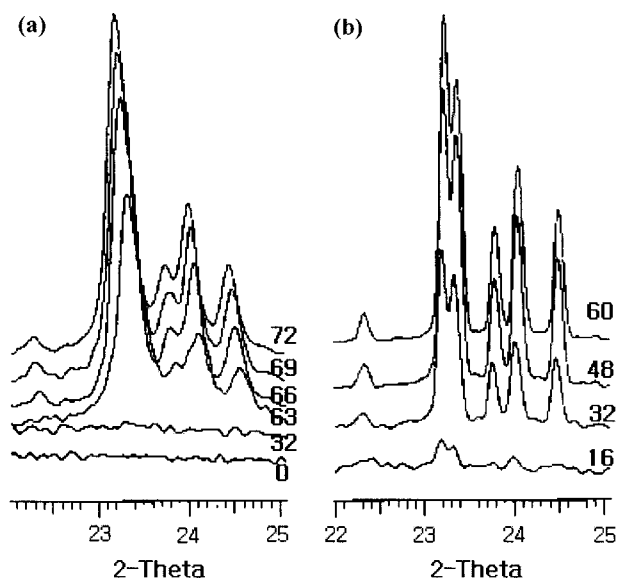


Fig. 5. X-ray diffraction patterns for products as a function of synthesis time.

(a) [Ga]-MFI, (b) ZSM-5

are shown in Fig. 3. In Fig. 3, both [Ga]-MFI and ZSM-5 exhibited a typical MFI structure [Argauer and Landolt, 1972; Gianetto et al., 1993]. ZSM-5 exhibited typical MFI peaks after 32 h, whereas the [Ga]-MFI exhibited after 63 h.

In Figs. 4 and 5, the XRD peaks of [Ga]-MFI shifted a little to a lower angle value (2θ) with the progress of crystallization, indicating a shift to a larger lattice space. This phenomenon may be due to the increase in the lattice parameters by the replacement of silicon atom with larger gallium atom, indicating the evidence of gallium substitution.

The crystallinity of ZSM-5 and [Ga]-MFI with synthesis time is shown in Fig. 6. ZSM-5 shows a typical S-type crystallization curve, whereas [Ga]-MFI does not clearly show the curve. [Ga]-MFI shows

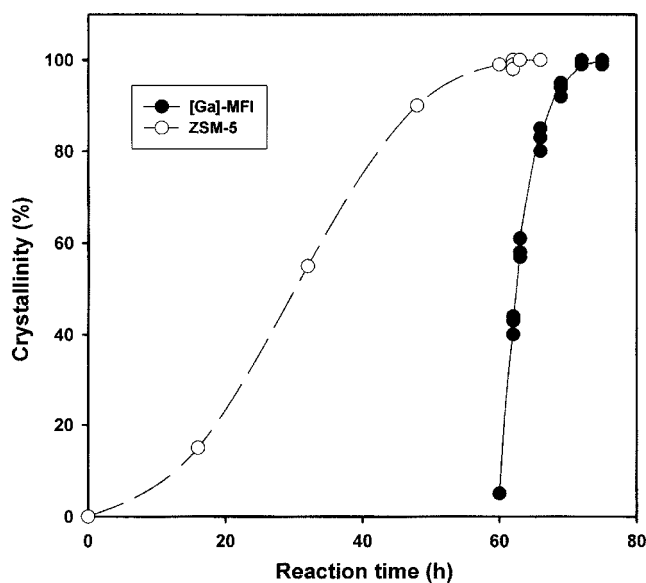


Fig. 6. Crystallinity of the [Ga]-MFI and ZSM-5 as a function of synthesis time.

a slower nucleation process (namely, a longer nucleation period) followed by a rapid crystal growth, while the ZSM-5 shows a gradual crystallization process. Oh et al. [2001] reported that one of the key factors in the crystallization of MFI-type zeolites is the action of OH^- ions. Erdem and Sand [1979] reported that the activation energy of the nucleation of ZSM-5 ($\text{Si}/\text{Al}_2=28$) is 5 times larger than that of the MFI-type silicalite (no aluminum, silicon only). He explained that this phenomenon is caused by the existence of aluminum that lowers the decomposition of the silica gel by consuming OH^- ions of the solution because of its 4-coordination numbers ($\text{Al}(\text{OH})_4^-$). Therefore, the longer nucleation period of the [Ga]-MFI in this study can be understood with the same reason mentioned above, that is, the gallium, with 6-coordination numbers, consumes more OH^- than the aluminum does.

2-3. Solid State *mas*-NMR

The identification of the existence of a substituted metal in a zeolite framework becomes possible with the use of solid-state *mas*-NMR. Fig. 7 shows the spectra of ^{71}Ga -*mas*-NMR with synthesis time. A single peak around 150 ppm, which corresponds to a chemi-

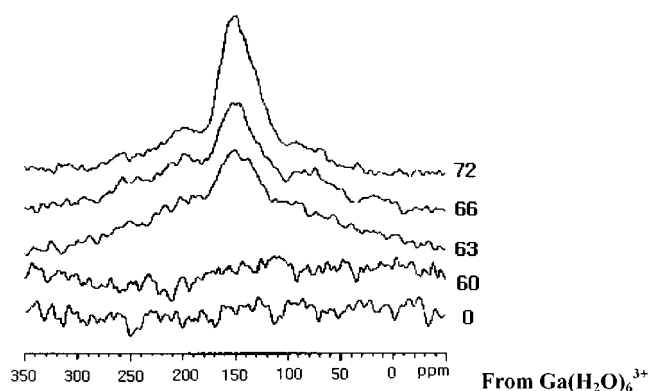


Fig. 7. ^{71}Ga *mas*-NMR spectra for products as a function of synthesis time.

cal shift from $\text{Ga}(\text{H}_2\text{O})_6^{3+}$, is observed. This is due to a chemical shift of the gallium coordinated tetrahedrally in the zeolite framework [Timken and Oldfield, 1987; Bayense et al., 1989]. The peak becomes larger with synthesis time, indicating the increase in the amounts of gallium incorporated into the lattice. Though gallium species in the initial gel-state were already confirmed by the XRF and XPS as summarized in Table 1, the peak (observed around 150 ppm) is not observed at the initial state in Fig. 7. This can be attributed to the fact that the detection of a non-tetrahedral gallium species is difficult because of its disorderliness [Bayense et al., 1989].

The ^{29}Si -*mas*-NMR spectra with synthesis time are shown in Fig. 8. The peaks for the $\text{Q}^4[\text{Si}(\text{OGa})]$ structure are observed in a range

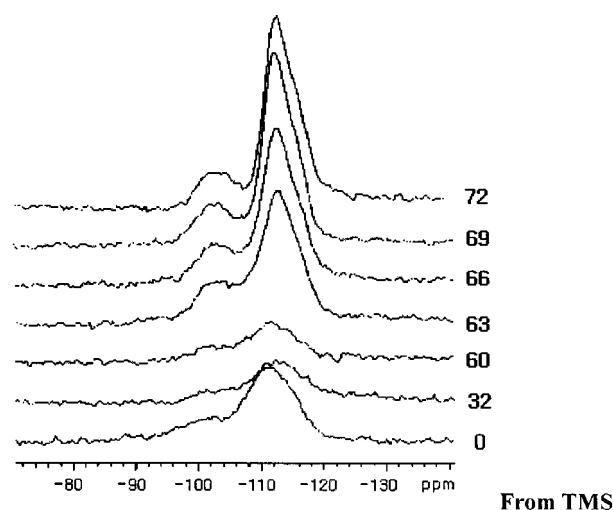


Fig. 8. ^{29}Si *mas*-NMR spectra for products as a function of synthesis time.

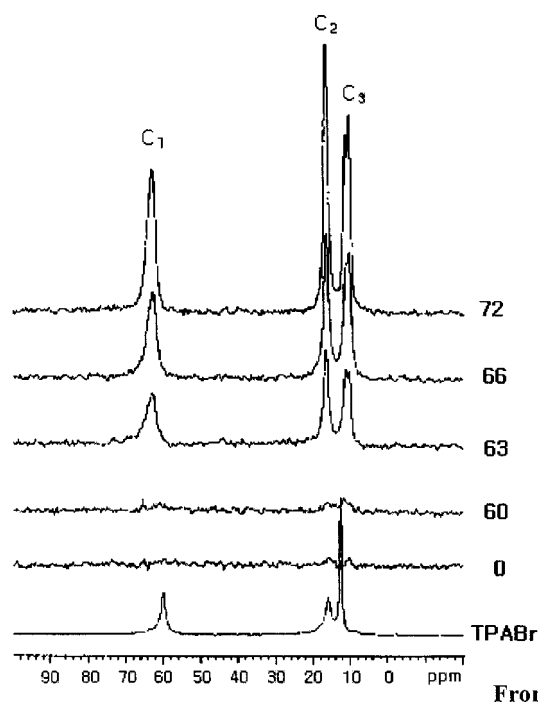


Fig. 9. ^{13}C *cpmas*-NMR spectra for products as a function of synthesis time.

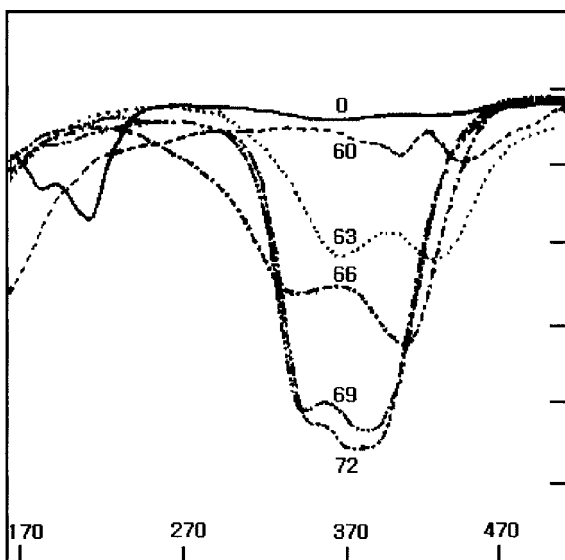


Fig. 10. DTG curves for products as a function of synthesis time.

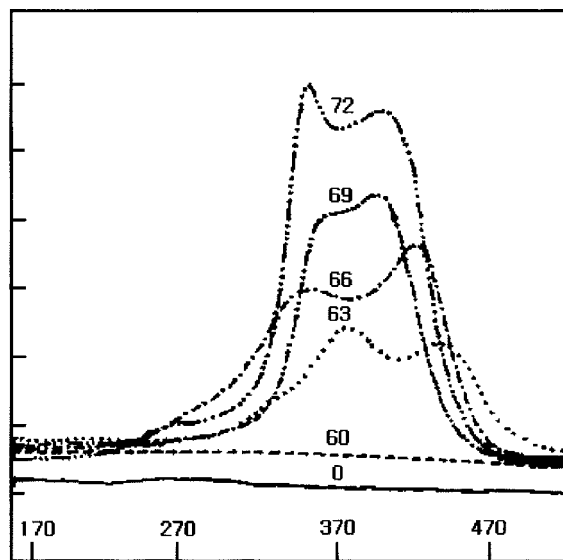


Fig. 11. DTA curves for products as a function of synthesis time.

of -98 – 120 ppm for all the synthesis time. After 63 h, the peaks for Si(OGa) and Si(1Ga) are also observed at -112 and -104 ppm, respectively [Lin and Klinowski, 1992].

The ^{13}C -*cpmas*-NMR spectra with the synthesis time are presented in Fig. 9. After 63 h, the peaks for the occluded organic template (TPA^+) are observed and progressively increased with the synthesis time. The intensity of the ^{13}C -*cpmas* NMR spectra is well consistent with the crystallinity results of XRD. Therefore, the inten-

sity of the ^{13}C -*cpmas*-NMR spectra can be used as a measure of the crystallinity of zeolites [Gabelica et al., 1983; Nagy et al., 1986]. The spectra for the occluded organic template are slightly shifted from the original TPABr. It has been known that the differences in the shifted peaks stem from a distortion of the symmetric TPA^+ ion in the porous zeolite structure and/or an interaction of the TPA^+ ion with the zeolite [Gabelica et al., 1983].

2-4. Thermal Analysis

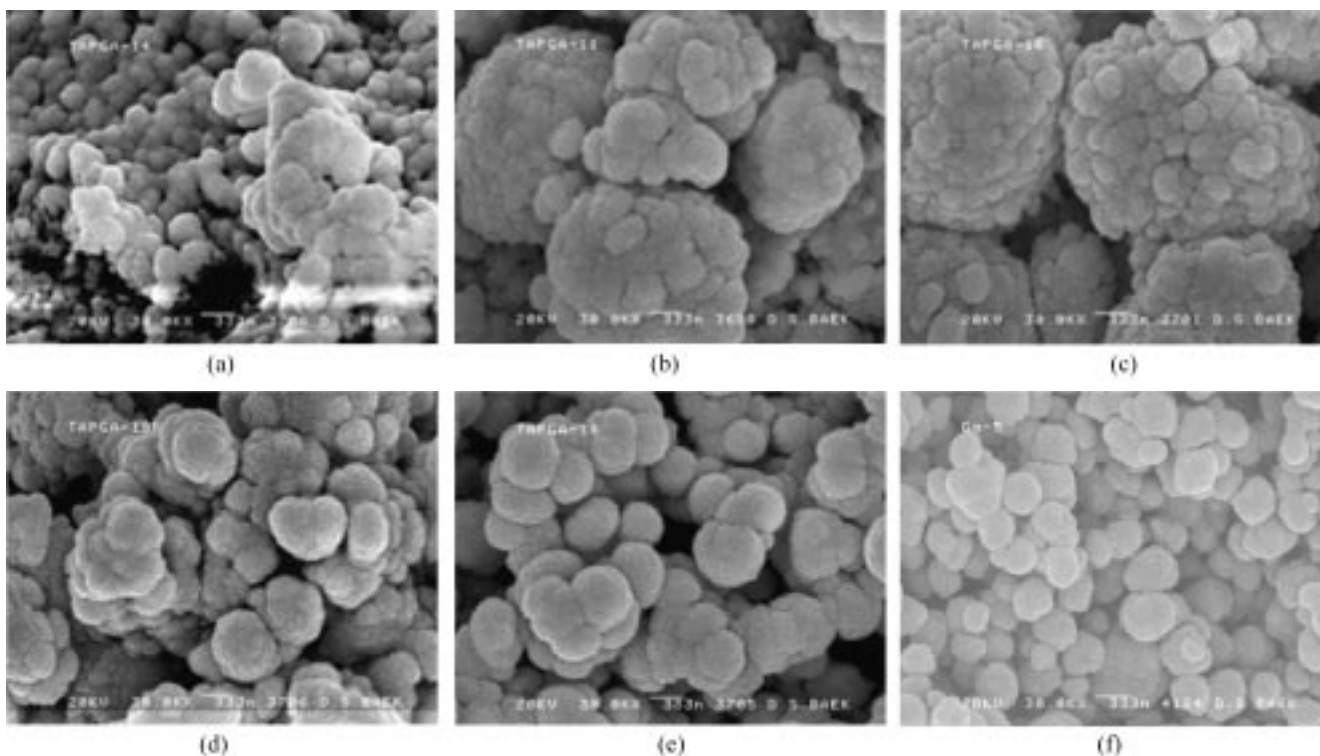


Fig. 12. SEM micrographs for products as a function of synthesis time.

(a) 0 h, (b) 32 h, (c) 60 h, (d) 63 h, (e) 66 h, (f) 72 h.

Thermal analyses of the products were carried out to get more information in relation to the ^{13}C -cpmas-NMR. The results are presented in Figs. 10 and 11. Both the weight loss and the heat evolution due to the removal of the organic template are observed at 280–450 °C in Figs. 10 and 11, respectively. The DTG and DTA curves clearly show the removal of the organic template after 63 h, and become more significant with the synthesis time, showing good accordance with the ^{13}C -cpmas-NMR results. The amount of organic template occluded in the structure was increased with the synthesis time, and the removal temperature of the organic template was lowered with the synthesis time. This phenomenon implies that the interaction between organic template and zeolite lattice becomes weak because of a stabilization of the zeolite structure with time.

3. Morphology Change

The changes in the morphology of the products with synthesis time were observed by using SEM; the results are shown in Fig. 12. Lumps of particles of various sizes were observed at the initial gel state, and they were progressively aggregated with synthesis time. However, from 63 h, the aggregated particles changed into particles having smaller sizes. The particle size distribution of the final products was analyzed. About 95% of the particles were in a range of 220–380 nm in size, while the remaining 5% of the particles were smaller than 50 nm. These sizes are relatively very small when compared with the particle sizes (1–7 μm) synthesized in autoclaves [Giannetto et al., 1993; Brabec et al., 1998].

CONCLUSION

The [Ga]-MFI was successfully synthesized under atmospheric pressure at 97 °C in 72 h. About 95% of the particles were in a range of 220–380 nm in size. The final products were verified to be a typical MFI-type zeolite. It was possible to verify the gallium species coordinated in zeolite framework by using ^{71}Ga -mas-NMR. It was found that the nucleation of the [Ga]-MFI took a quite long time, while the crystallization occurred very fast. It is supposed that the nucleation is a rate-controlling step in the [Ga]-MFI synthesis under atmospheric pressure. Therefore, if the induction period of nucleation can be shortened, it would be possible to synthesize the [Ga]-MFI commercially under atmospheric pressure.

REFERENCES

- Argauer, R. J. and Landolt, G. R., US. Patent, **3**, 702886 (1972).
- Bayense, C. R., Van Hooff, J. H. C., Kentquens, A. P. M., DeHaan, J. W. and Van de Ven, L. J. M., "The Removal of Gallium from the Lattice of MFI-gallosilicates as Studied by Gallium-71 MAS-NMR Spectroscopy," Proceedings of the 8th International Zeolite Conference, 105 (1989).
- Bayense, C. R., van der Pol, A. J. H. P. and van Hoff, J. H. C., "Aromatization of Propane over MFI-gallosilicates," *Appl. Catal., A*, **72**, 81 (1991).
- Brabec, L., Jeschke, M., Klik, R., Novakova, J., Kubelkova, L. and Freude, D., "Various Types of Ga in MFI Metallosilicates Characterization and Catalytic Activity," *Appl. Catal., A*, **167**, 309 (1998).
- Cambor, M. A., "Synthesis and Characterization of Gallosilicates and Galloaluminosilicates Isomorphous to Zeolite Beta," *J. Zeolites*, **12**, 280 (1992).
- Chiyoda Corp., JP05269385 (1993).
- Choudhary, V. R., Devadas, P., Kinage, A. K., Sivadinarayana, C. and Guisnet, M., "Pulse Reaction Studies on Variations of Initial Activity/Selectivity of O_2 and H_2 Pretreated Ga-modified ZSM-5 Type Zeolite Catalysts in Propane Aromatization," *J. Catal.*, **158**, 23 (1996).
- Choudhary, V. R., Kinage, A. K. and Guisnet, M., "Acidity, Catalytic Activity, and Deactivation of H-gallosilicate (MFI) in Propane Aromatization: Influence of Hydrothermal Pretreatments," *J. Catal.*, **158**, 537 (1996).
- Choudhary, V. R. and Kinage, A. K., "Hydrothermal Synthesis of Galloaluminosilicate (MFI) Zeolite Crystals Having Uniform Size, Morphology and Ga/Al Ratio," *Zeolites*, **18**, 274 (1997).
- Erdem, A. and Sand, L. B., "Crystallization and Metastable Phase Transformations of Zeolite ZSM-5 in the $(\text{TPA})_2\text{O}$ -sodium Oxide-potassium Oxide-aluminum Oxide-silicon Dioxide-Water System," *J. Catal.*, **60**, 241 (1979).
- Gabelica, Z., Nagy, J. B. and Debras, G., "Characterization of x-ray Amorphous ZSM-5 Zeolites by High Resolution Solid State Carbon-13 NMR Spectroscopy," *J. Catal.*, **84**, 256 (1983).
- Giannetto, G., Monque, R., Perez, J. and Garcia, L., "Comparison of Crystallization Rates of [aluminum]- and [gallium]-MFI-type Zeolites," *Zeolites*, **13**, 557 (1993).
- Giannetto, G., Montes, A., Gnep, N. S., Florentino, A., Cartraud, P. and Guisnet, M., "Conversion of Light Alkanes into Aromatic Hydrocarbons. VII. Aromatization of Propane on Gallosilicates: Effect of Calcination in Dry Air," *J. Catal.*, **145**, 86 (1993).
- Gnep, N. S., Doyemet, J. Y. and Guisnet, M., "Creation of Mesopores in Monodimensional Zeolites. A Way of Improving Their Catalytic Stability," *Stud. Surf. Sci. Catal.*, **46**, 153 (1989).
- Gnep, N. S., "Effects of Steaming on the Shape Selectivity and on the Acidity of HZSM-5," *J. Mol. Catal.*, **45**, 281 (1998).
- Guisnet, M., Gnep, N. S. and Alario, F., "Aromatization of Short Chain Alkanes on Zeolite Catalysts," *Appl. Catal., A*, **89**, 1 (1992).
- Inui, T., Makino, Y., Okazumi, F., Nagano, S. and Miyamoto, A., "Selective Aromatization of Light Paraffins on Platinum-ion-exchanged Gallium-silicate Bifunctional Catalysts," *Ind. Eng. Chem. Res.*, **26**, 647 (1987).
- Kanai, J. and Kawata, N., "Aromatization of Hexane over Galloaluminosilicate and Allosilicate," *Appl. Catal., A*, **55**, 115 (1989).
- Khodakov, A. Y., Kustov, L. M., Bondarenko, T. N., Dergachev, A., Kazansky, V. B., Minachev, K. M., Borbely, G. and Beyer, H. K., "Investigation of the Different States of Gallium in Crystalline Gallosilicates with Pentasil Structure and Their Role in Propane Aromatization," *Zeolites*, **10**, 603 (1990).
- Kim, W. G., Kim, J. H., Ahn, B. J. and Seo, G., "The Skeletal Isomerization of C-4-C-7 1-Olefins over Ferrierite and ZSM-5 Zeolite Catalysts," *Korean J. Chem. Eng.*, **18**, 120 (2001).
- Lee, G. D., Han, T. J. and Lee, H. I., "Gas-phase Isomerization of Ethylbenzene over Pt-Heteropoly Acid/Zeolite Catalysts," *Korean J. Chem. Eng.*, **3**, 53 (1986).
- Lee, K. H. and Ha, B. H., "Catalytic Cracking of Vacuum Gas Oil on Alumina/Zeolites Mixtures-effects of Precipitation pH of Alumina and Zeolite Type on Product Distribution," *Korean J. Chem. Eng.*, **15**, 533 (1998).
- Lin, X. S. and Klinowski, J., "Acidic Hydroxyl Groups in Zeolites X and Y: a Correlation between Infrared and Solid-state NMR Spectra," *J. Phys. Chem.*, **96**, 3403 (1992).

- Meriaudeau, P. and Naccache, C., "The Role of Ga₂O₃ and Proton Acidity on the Dehydrogenating Activity of Ga₂O₃-HZSM-5 Catalysts: Evidence of a Bifunctional Mechanism," *J. Mol. Catal.*, **59**, L31 (1990).
- Mitsubishi Chem. Corp., JP09020706 (1997).
- Mobil Oil Corp., EP187496 (1986).
- Mobil Oil Corp., EP327189 (1989).
- Nagy, J. B., Bodart, P., Derouane, E. G., Gebelica, Z. and Nastro, A., "Role of Alkali and Tetrapropylammonium Cations in (M)ZSM-5 Hydrogel Precursors," Proceedings of the 7th International Zeolite Conference, 231 (1986).
- Oh, H. S., Kang, K. K., Kim, M. H. and Rhee, H. K., "Synthesis of MFI-type Zeolites under Atmospheric Pressure," *Korean J. Chem. Eng.*, **18**, 113 (2001).
- Shapiro, E. S., Shevchenko, D. P., Tkachenko, O. P. and Dmitriev, R. V., "Platinum Promoting Effects in Pt/Ga Zeolite Catalysts of Lower Alkane Aromatization. I. Ga and Pt Electronic States, Dispersion and Distribution in Zeolite Crystals in Dependence of Preparation Techniques. Dynamic Effects Caused by Reaction Mixture," *Appl. Catal., A*, **107**, 147 (1994).
- Simmons, D. K., Szostok, R., Agrawal, P. K. and Thomas, T. L., "Gallosilicate Molecular Sieves: the Role of Framework and Nonframework Gallium on Catalytic Cracking Activity," *J. Catal.*, **106**, 287 (1987).
- Szostak, R., "Molecular Sieve - Principles of Synthesis and Identification," 197 (1988).
- Thomas, J. M. and Liu, X. S., "Galloseolite Catalysts: Preparation, Characterization and Performance," *J. Phys. Chem.*, **90**, 4843 (1986).
- Timken, H. K. C. and Oldfield, E., "Solid-state Gallium-69 and Gallium-71 Nuclear Magnetic Resonance Spectroscopic Studies of Gallium Analog Zeolites and Related Systems," *J. Am. Chem. Soc.*, **109**, 7669 (1987).
- Vaw ver Aluminium Werke Ag., DE4021118 (1992).
- Yakerson, V. I., Vasina, T. V., Lafer, L. I., Sytnyk, V. P., Dylch, G. L. and Mokhov, A. V., "The Properties of Zinc and Gallium Containing Pentasils - the Catalysts for the Aromatization of Lower Alkanes," *Catal. Lett.*, **3**, 339 (1989).